

## CHAPTER 34

### VELOCITY AND PRESSURE FIELD OF SPILLING BREAKERS

M.J.F. Stive<sup>1)</sup>

#### ABSTRACT

The internal velocity and pressure fields of quasi-steady spilling breaking waves have been investigated experimentally. The internal flow fields are shown to be in qualitative agreement with a model proposed by Peregrine and Svendsen (1978). Furthermore a quantitative comparison is made with non-breaking wave theories. Measurements of the pressure field are presented, and interpreted semi-quantitatively using the vertical momentum balance. Finally, it is shown how the integral properties can be obtained and analysed.

#### I. INTRODUCTION

The surfzone water motion is a topic that deserves and receives a lot of theoretical and experimental investigation. However, in experimental studies of the surf zone measurements have generally been restricted to the external characteristics, i.e. the instantaneous and time mean surface elevations. It is conspicuous that the internal kinematics of breaking waves have received little experimental attention. It is also conspicuous that the experimental study of the energy dissipation and the momentum flux variation is literally "superficial". Based on measurements of the internal kinematics and dynamics a more fundamental approach is possible, e.g. gradients in the momentum flux can be related to variations in mean water level, and gradients in the energy flux can provide the local energy dissipation. At the same time it may be possible to relate the turbulence intensity to the energy dissipation (Battjes, 1975).

Along the lines indicated above an experimental study was initiated of the internal velocity and pressure field of waves breaking on a gentle slope. The experimental data from this study are analysed in two consecutive phases. The first phase concentrates on instantaneous values. The second phase concentrates on integral properties, i.e. the densities and fluxes of momentum and energy, and on the energy dissipation in relation to the measured turbulence.

This paper presents an indication of the results obtained so far. A more extensive presentation of the results will follow.

Following Svendsen et al (1978) a characteristic description of the surfzone water motion is given in §3. The kinematics are described in §4, in which the model for the flow field of a quasi-steady breaking wave as proposed by Peregrine and Svendsen (1978) is shown to agree with the experimental results. Furthermore the measurements are compared to non-breaking wave theories. A semi-quantitative description of the dynamics is given in §5. Finally, the planned evaluation of the integral properties is outlined in §6 and illustrated with a preliminary result.

---

<sup>1)</sup>Project Engineer, Harbours and Coasts Branch, Delft Hydraulics Laboratory, The Netherlands.

## 2. EXPERIMENTS

### *Arrangements*

The experiments were conducted in a wave flume of the Delft Hydraulics Laboratory. The flume is 55 m long, 1 m wide and 1 m high.

Regular waves without free second harmonic components were generated in a water depth of 0.85 m. To obtain a control signal for the wave generator which resulted in a maximum suppression of the free second harmonics a simple trial and error procedure was applied, using Fontanet's theory (see e.g. Hulsbergen, 1974) as a first approximation.

To enable the construction of instruments in the bottom of the horizontal section a false, concrete floor was made, which reduced the water depth of the horizontal section to 0.70 m. The waves broke on a plane, concrete beach of a 1:40 slope (see Fig. 1a).

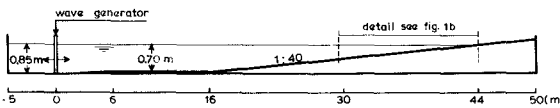


Figure 1a Experimental set-up

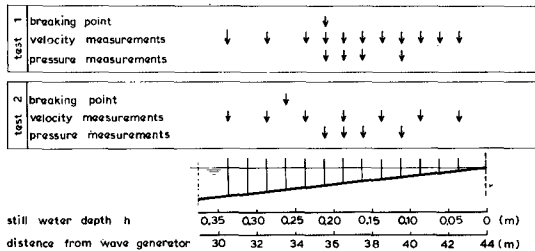


Figure 1b Detail experimental set-up

### *Measurements*

The surface variations, i.e. the time mean and instantaneous vertical elevations of the surface, were measured over the whole length of the flume at positions with an interval of 1 m by means of resistance type wave gauges. Velocities of propagation were determined from the time of propagation of characteristic points of the wave surface between these positions.

It must be noticed, that resistance type wave gauges in principle cannot be used in the aerated region of breaking waves. Awaiting the results of a study of this aspect the conclusions of the study of Svendsen et al (1978) were used, i.e. (1) the wave gauges measure solid water and (2) the actual air content in the most densely entrained laboratory wave is only 2-4 percent. Thus, in view of the required accuracies the measured surface elevations are regarded as the elevation of water with normal density.

The horizontal and vertical component of velocity were measured by means of a laser doppler velocimeter, which is described elsewhere (Godefroy, 1978). The measurements were concentrated on the breaking and the near-breaking zone (see Fig. 1b). They were conducted at different levels between bottom and surface elevation.

It must be noticed, that during measurements the doppler signal may drop out temporarily for several reasons, such as the presence of air bubbles or large opacities. When the doppler signal drops out the last detected doppler frequency is held until the next doppler burst of about the same frequency is detected. Consequently these drop-outs occur when measuring above the level of the wave troughs and in water with entrained air as found in the front of breaking waves. Concerning the latter case it can be remarked that in view of the procedure of signal processing measurements are meaningless if the time scale of the drop-outs exceeds the time scale of the turbulent fluctuations. The time scale of the drop-outs increases with the density of the aeration. As a consequence measurements are only possible up to lightly aerated regions.

Pressures were measured by means of differential pressure transducers (0.8 cm diameter) at only four positions in the breaker zone (see Fig. 1b). In each of these positions the transducers were mounted at different elevations in a transparent, dummy side wall.

Symbol and sign conventions are as follows. The surface elevation is denoted  $\eta$ , the horizontal velocity component  $u$ , the vertical velocity component  $w$  and the pressure  $p$ . The horizontal  $x$ -axis is positive in the direction of wave propagation. The vertical  $z$ -axis is positive upwards, while the  $z$ -origin is chosen at the still water level.

Because of the exploratory nature of the investigation the experiments were restricted to two wave conditions, which are referred to as test 1 and test 2. The wave characteristics are as follows:

	$H_o$ (m)	$H_{\text{hor. section}}$ (m)	$T_{\text{wave maker}}$ (m)	$H_{\text{breaker}}$ (m)	$H_o/L_o$ (-)
test 1	0.159	0.145	1.79	0.178	0.032
test 2	0.142	0.145	3.00	0.226	0.010

The breaking behaviour at the breaking point of test 1 falls in the category "spilling breaking", while that of test 2 falls in the category "plunging breaking".

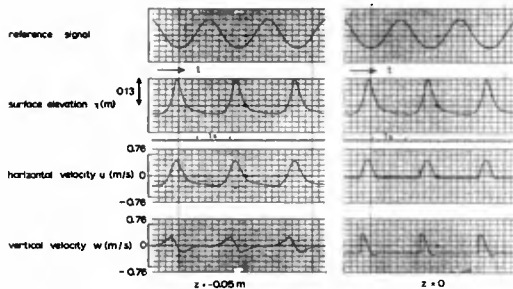


Figure 2a Typical recording near-breaking region (test 1,  $x = 34.5$  m)

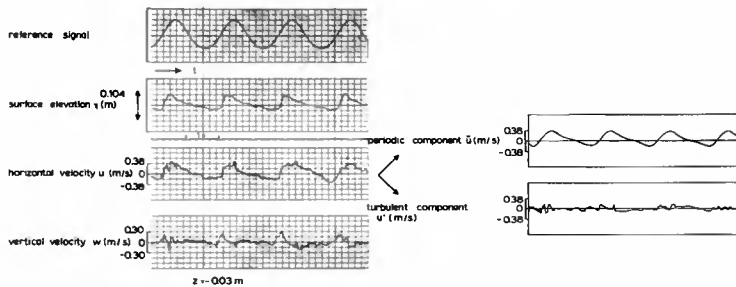


Figure 2b Typical recording breaking region (test 1,  $x = 38.5$  m)

#### Procedures

Typical recordings of the surface elevation and the velocity components in the near-breaking and the breaking region (see Fig. 2a and 2b) show that the non-breaking wave motion is a purely periodic quantity, and that the breaking wave motion is a fluctuating quantity with a quasi-periodic character. To describe the breaking motion it is considered as the sum of a purely periodic component (indicated by a tilde) and a non-periodic residual component (indicated by a dash). The periodic component is obtained by averaging the signals at a fixed phase of the reference signal, i.e. the command signal of the wave generator. This procedure may be described as ensemble averaging. The major part of the residual component is formed by the turbulent fluctuations of the breaking process and is therefore termed the turbulent component. These fluctuations are non-stationary in time. Because of their time-scale a recording over say  $n$  waves may be considered as  $n$  independent recordings of the turbulent process. From this ensemble an estimate of e.g. the r.m.s.-value at a fixed time may be obtained.

Summarising, the non-breaking wave motion can be fully described just by a periodic component, i.e.  $\eta = \bar{\eta}$ ,  $u = \bar{u}$ ,  $w = \bar{w}$  and  $p = \bar{p}$ . The breaking wave motion can be described as the sum of a periodic and a "turbulent" component, i.e.  $\eta = \bar{\eta} + \eta'$ ,  $u = \bar{u} + u'$ ,  $w = \bar{w} + w'$  and  $p = \bar{p} + p'$ .

The periodic components are obtained as the ensemble mean over a minimum of 20 waves. The r.m.s.-value of the turbulent component at a fixed phase is obtained from the ensemble of minimum 20 "recordings" of the turbulent process. The time mean value of the turbulent component is zero by its definition. Consequently, the time mean value of the wave motion is equal to the time mean value of the periodic wave motion, i.e.  $\bar{\eta} = \bar{\eta}$ ,  $\bar{u} = \bar{u}$ ,  $\bar{w} = \bar{w}$  and  $\bar{p} = \bar{p}$ , where an overbar indicates time-averaging over an integral number of wave periods. Furthermore, for points above the level of the wave troughs which are not always submerged,  $u$ ,  $w$  and  $p$  are zero by definition when  $z > \eta(x, t)$ , while their time mean value is the time mean over an integral number of full wave periods.

At each of the indicated positions the velocities and the pressures at the different levels were measured consecutively, i.e. non-simultaneously. Simultaneously with a velocity or pressure measurement at a certain level the command signal of the wave generator and the surface elevation were recorded. Using these signals as a reference it is possible to couple the non-simultaneous measurements in one cross-section. This procedure of composing the velocity and pressure fields introduces inaccuracies due to the determination of the wave motion from an ensemble of a limited number of waves. These inaccuracies are found to be of the order of  $\pm 2 - 3\%$  of the maximum periodic value. They exceed the instrumental inaccuracies, with the exception of inaccuracies due to drift of the laser doppler velocimeter and the pressure transducers, amounting to  $\pm 1$  cm/s and  $\pm 0.2$  cm ( $H_2O$ ) respectively.

### 3. CHARACTERISTIC DESCRIPTION

This study is restricted to the kind of breaking waves that are usually found on gently sloping, sandy beaches with relatively wide breaker zones. A characteristic description of the breaking wave motion on these beaches is given by Svendsen et al (1978). They differentiate between a so-called outer and inner region (see Fig. 3). In the outer region the initial, chaotic breaking (ranging from spilling to plunging) takes place over a relatively short horizontal distance of several times the waterdepth at the breaking point. In the inner region soon a relatively well organized motion develops. The breaking motion is fully turbulent, while the mean motion is quasi-steady. A definition of a quasi-steady wave is given by Peregrine and Svendsen (1978): "one which changes little during the time a water particle takes to pass through it, excluding water particles which may become trapped in a surface roller". At this stage of its breaking motion a breaker on a beach may be described as a spilling breaker or bore. In case the depth continues to decrease the quasi-steady breaking motion is maintained until the shoreline is reached.

Indeed, the remarkable feature of the inner region is that the wave shapes throughout this region are very similar, as a comparison of the dimensionless surface profiles of the inner region shows (see Fig. 6 and 8). This conservation of wave shape is also illustrated by the tendency of the velocities

of propagation of characteristic points of the wave front to coincide as the waves propagate into the inner region (see Fig. 4). Comparison of the wave shapes for test 1 and test 2 shows that the similarity also holds for waves at the same position originating from different deep water conditions.

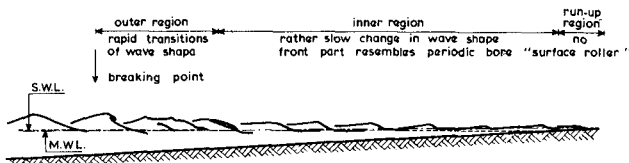


Figure 3 Wave characteristics in the surfzone (after Svendsen et al., 1978)

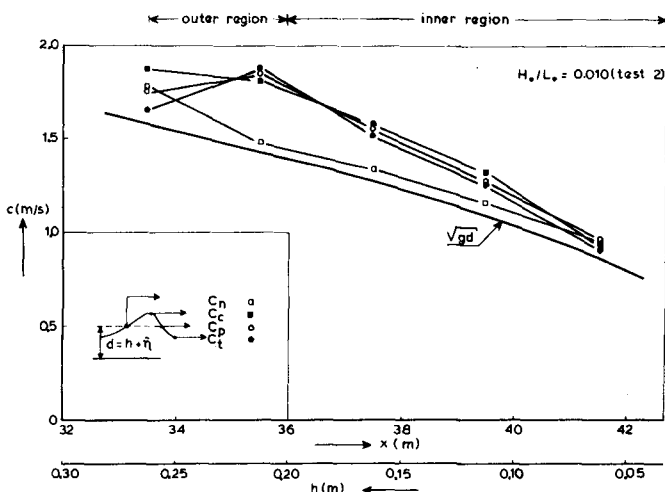


Figure 4 Velocities of propagation

From the surface variations it can be concluded that the water motion at each depth seems to be strongly locally controlled. Local depth and bed slope determine the characteristics of flow and hence the shape of the wave, including the energy flux, the energy dissipation and consequently the decrease in wave height. This hypothesis finds support in the nearly constant ratio of

wave height over mean water depth  $H/d$  for both tests (see Fig. 5), which is used to define the extent of the inner region.

In the next paragraph it is shown that the flow fields of the inner breaking region confirm the hypothesis of similarity with regard to the water motions.

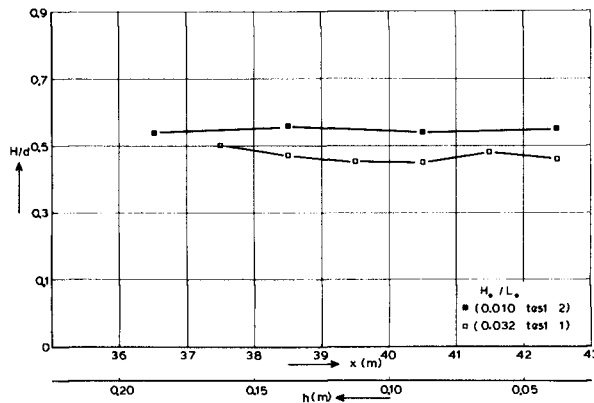


Figure 5 Variation of wave height to water depth ratio

#### 4. HORIZONTAL VELOCITY FIELD

The measured velocity fields presented and analysed in this paragraph belong to the inner breaking region. Because of the quasi-steady motion in this region it is possible to interpret the measured motion as being of waves of constant form. Virtually no velocity measurements were conducted in the relatively small outer region. The violent variation of the water motions in this region prohibits a constant form interpretation, so that for an analysis detailed spatial measurements would be required.

##### *Comparison with non-breaking wave theories*

The measured periodic velocity fields are compared to the theoretical fields for non-breaking waves of constant form to check the applicability of these theories, since they are commonly used for lack of breaking wave theories.

The selection of the theories used for the comparison is mainly based on the recommendations of the study of LeMéauté et al (1968), because the experimental wave characteristics of their study are close to the experimental characteristics at the different measuring positions of both tests of this

study. In the study by LeMéhauté et al (1968) a number of theories were used for comparison with measured horizontal velocities under the wave crest. Dean (1974) extended the comparison with the stream function method. Of the 12 theories included in the comparison the stream function theory provided the best agreement followed in order by Goda's empirical formula, the cnoidal theory of Keulegan and Patterson and linear theory. Since Dean's stream function theory requires interpolation from tables and since Goda's formula is empirical, it was at this stage of the study decided to use the third and fourth best theories, viz. the cnoidal theory of Keulegan and Patterson (Masch and Wiegel, 1964) and the linear theory.

Firstly, the measured horizontal periodic velocity fields for test 1 are compared with the theoretical cnoidal fields (see Fig. 6). Secondly, the measured maximum (shoreward) and minimum (seaward) horizontal periodic velocities for both tests are compared with the extreme velocities following from the cnoidal and linear theory (see Fig. 7). Thirdly, in the same figure the measured time mean horizontal velocities are compared to the cnoidal and linear time mean velocities.

For both tests a number of representative results for the breaking waves in the inner region is presented. For comparison also a near-breaking wave is included. Vertical distances are made dimensionless by the local mean water depth, horizontal distances by the wave length and time by the wave period. It is noticed that the origin of the vertical z-axis is at the still water level. The horizontal lines indicate the levels at which the measurements were conducted. On the basis of these measurements fields with lines of equal velocities are constructed. The positive time axis of the measured velocity fields is directed to the right, so the wave profiles "propagate" to the left. It is stressed that the measured velocities are Eulerian velocities.

For both the cnoidal and linear theory two different formulations are used. The unbracketed values in Figure 6 and the full curves in Figure 7 are for the usual formulation in which the frame of reference is chosen such that the mean horizontal momentum or mass flow under the level of the wave troughs is zero:  $-h \int_{t_0}^{t_1} \rho u dz = 0$ . The in-phase relation of surface elevation and horizontal velocity introduces a net mass flow or Eulerian mass transport in the region above the level of the wave troughs. Since the measurements were conducted in a closed wave flume in a stationary situation the total mean mass flow is zero:  $-h \int_{t_0}^{t_1} \rho u dz = 0$ . Therefore a second formulation is chosen, such that the net shoreward mass flow in the region above the wave troughs equals the net seaward mass flow in the region below the troughs. This formulation is simply found by changing the speed of the frame of reference by the amount  $-\eta_t \int_{t_0}^{t_1} \rho u dz / \partial t$ . The results are given by the bracketed values in Fig. 6 and the dashed curves in Fig. 7.

It is noticed that for an irrotational wave motion, which is spatially homogeneous (apart from phase differences), the mean mass flow under the wave troughs is essentially constant. The "conduction solution" of Longuet-Higgins (1953) for rotational wave motion in a viscous fluid of finite depth predicts a mean mass flow which is maximum seaward right below the level of the wave troughs but which changes to a shoreward mass flow near the bottom.

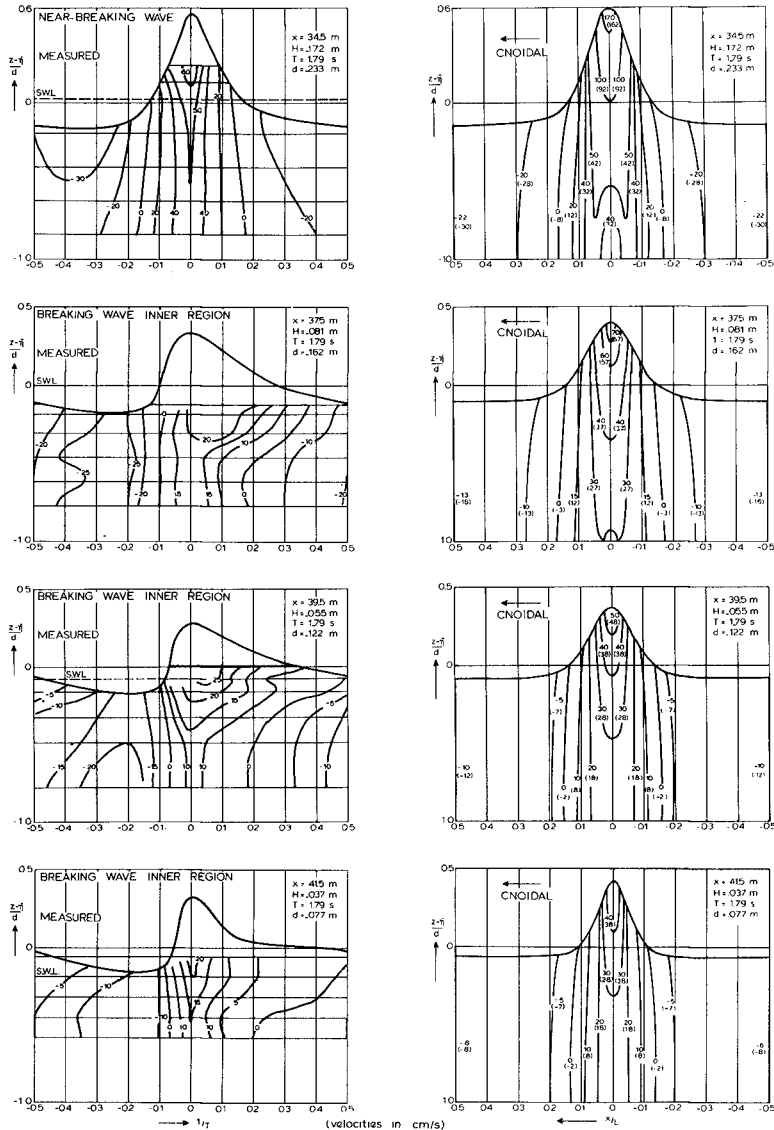


Figure 6 Comparison of measured and theoretical (cnoidal) horizontal periodic velocity fields of test I (see text for explanation)

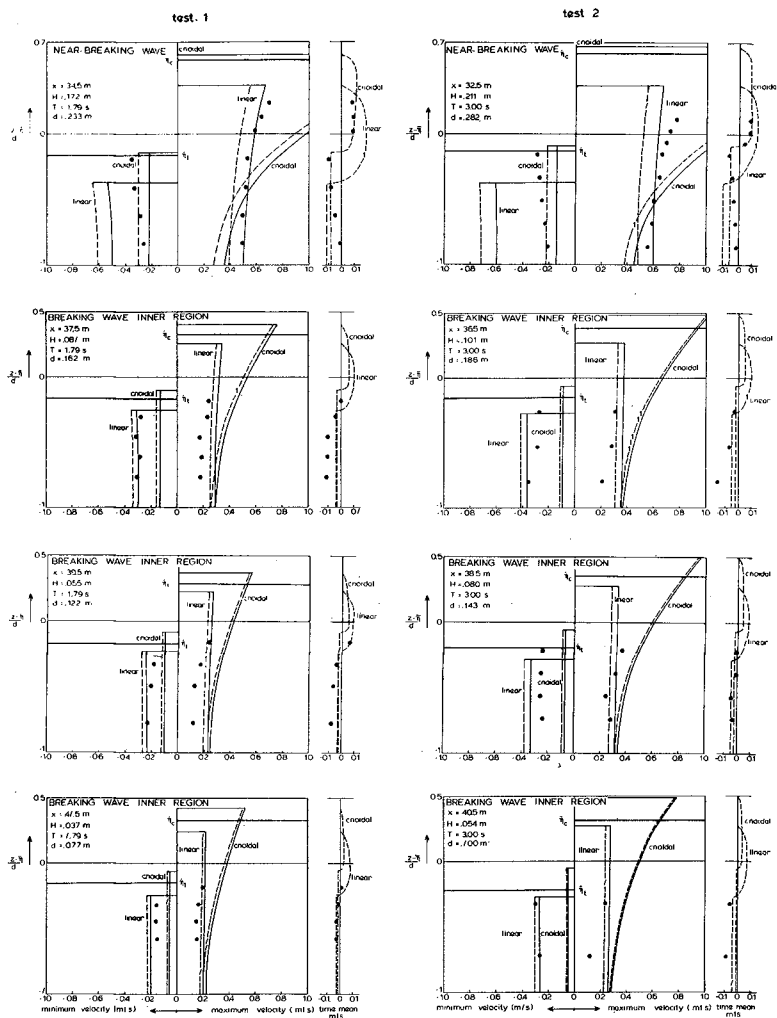


Figure 7 Comparison of measured and theoretical extreme horizontal periodic velocities for both tests (see text for explanation)

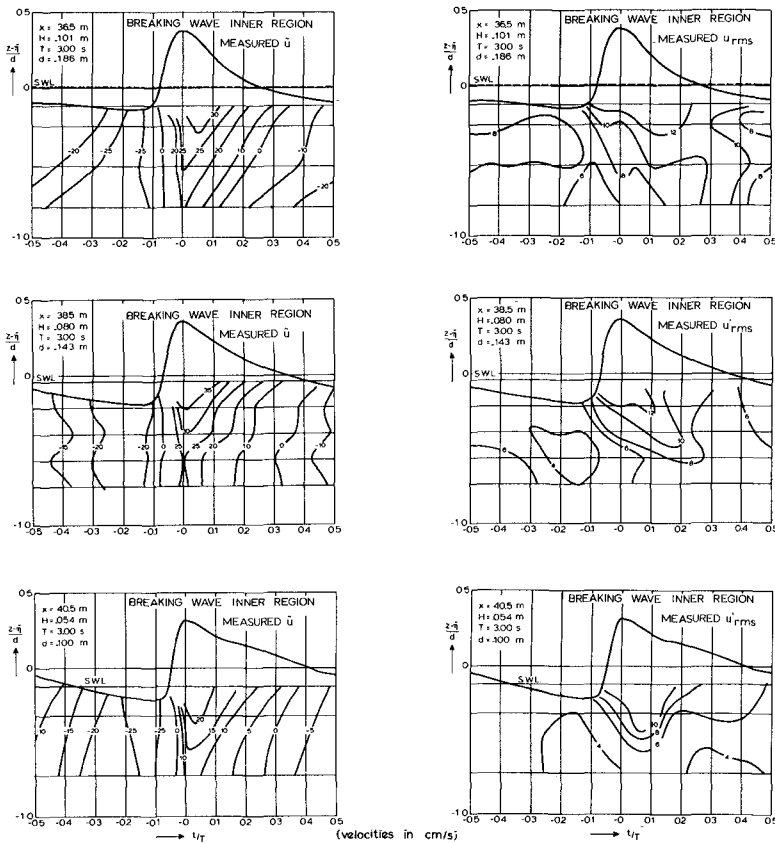


Figure 8 Measured horizontal periodic and turbulent velocities of test 2

Lagrangian measurements of Russell and Osorio (1958) in a closed wave flume confirmed this picture for non-breaking waves and found it to hold even for a sloping bottom.

From the comparison relating to the near-breaking waves (top of Fig. 6 and 7), it can be noted that:

- the surface elevation and the orbital wave motion remain quite symmetric horizontally,

- the surface elevation is well predicted by the cnoidal theory,
- the horizontal velocity is qualitatively and, with the exception of the upper crest region, quantitatively well predicted by the cnoidal theory,
- the discrepancies between the theoretical and measured maximum and minimum velocities are of the same order of magnitude as found by LeMéhauté et al. (1968),
- the time mean horizontal motion shows the tendencies as described by Longuet-Higgins' "conduction solution" (1953).

From the comparison relating to the breaking waves of the inner region (lower part of Fig. 6 and 7) it can be noted that

- the surface elevation and the orbital water motion are quite asymmetric horizontally and vertically,
- the cnoidal theory (for symmetric waves) is not able to predict the horizontal velocity field,
- the linear maximum and minimum horizontal velocities compare favourably to the measured extreme velocities,
- the net seaward flow below the wave troughs does not tend to zero or to shoreward flow near the bottom.

Figures 6 and 8 show that the horizontal periodic velocity fields of the inner breaking region for both tests and for different positions show a similar pattern that can be characterised as follows: in the regions just before the bore front arrives and in the lower regions a vertically homogeneous orbital motion exists which shows a horizontal asymmetry as can be expected from a non-breaking wave theory based on a similar asymmetric wave profile. Just behind the bore front a disturbed region exists, which seems to restore itself to a smooth velocity profile just before the next wave front arrives. The nature of these flow fields is described by the following model.

#### *A model for the flow field*

Based on visual observation Peregrine and Svendsen (1978) developed a model of a quasi-steady breaking wave (see Fig. 9a), which is briefly outlined below. The flow fields resulting from this model are compared to the measured flow fields of the inner breaking region.

At the front face of a spilling breaker an aerated surface layer can be observed, which is rapidly mixed into an increasing volume of aerated flow by the strong turbulence. The aerated flow commences at the toe of the aerated surface layer and forms a wedge. Longuet-Higgins and Turner (1974) describe the surface layer as a roller, falling down the front face of the wave. It is doubted, whether the surface layer can be treated as a roller separate from the region of highly turbulent flow. Peregrine and Svendsen (1978) hypothesize that it acts as a trigger to initiate the turbulence and that the initial volume of turbulent flow resembles a turbulent mixing layer.

The influence of gravity limits the development of the mixing layer region strongly, due to the absence of an upper fluid. A substantial part of the aerated, turbulent flow is found behind the mixing region, where the flow is like that in a wake. In this wake region the turbulence spreads and decays.

The horizontal velocity field resulting from this model is sketched in Figure 9b, for a frame of reference moving with the wave. The uniform flow approaching the breaking wave meets the toe of the surface roller, which has a velocity not very different from zero. In the moving reference frame the uniform velocity of the undisturbed flow is of the order of the propagation velocity  $c$  to which the oscillatory motion of order of  $0.1 - 0.2 c$  is added. The mixing layer region develops in which the uniform velocity of the lower fluid changes to the zero velocity of the surface layer until the influence of gravity becomes dominant. In the wake region the uniform velocity of the undisturbed lower regions is slowly restored over the whole depth.

In figure 9c the velocity field described above is translated to a field with isolines of horizontal velocity for a fixed frame of reference. Comparison of this typical velocity field with the presented measured periodic flow fields (Fig. 6 and 8) shows that the model of the flow field agrees encouragingly well with the measured flow fields. However, the lack of measurements in the most aerated regions restricts this conclusion to the far wake region and the lower boundaries of mixing region and initial wake region.

Turbulent mixing layers grow linearly with distance in a wedge. The growth rate depends primarily on the velocity difference of the meeting flows. Brown and Roshko (1974) present values for the visually observed growth rate for a range of velocity differences including the case where the upper fluid velocity is zero. The measured flow fields (Fig. 6 and 8) give an indication of the lower boundary of the mixing layer. Since the model assumes the surface elevation to be the upper boundary, it is possible to obtain the growth rate of the mixing regions of the flow fields measured at the different positions in the inner breaking region. These growth rates are compared (see Fig. 10) to the values which Brown and Roshko present for their cases  $u_2 = 0$ ,  $\rho_2/\rho_1 = 1$  and  $u_2 = 0$ ,  $\rho_2/\rho_1 = 1/7$ , in which the subscripts 1 and 2 stand for the lower and upper fluid respectively. Although the measurements on which these values are based show a considerable scatter, which is also true for the presented growth rates, it is concluded that there is a fair order of magnitude agreement. The density difference that Brown and Roshko introduced in their experiments appears to create only quantitative differences. Because of the scatter in the measured growth rates presented in Fig. 10 it is not possible to perceive any effects of a lower mean density of the surface layer due to air entrainment.

Finally, it is shown that also the measured horizontal turbulent velocity field ( $u'_{r.m.s.}$ ) is in agreement with the model. For positions corresponding to the measured periodic velocity fields of Figure 8 some typical examples are given in the same figure. The lower boundary of the mixing region is indicated by the spreading of the high intensities of the turbulence. In the wake region behind the mixing zone a decay of the turbulent intensities is clearly observed. It is noticed that the velocity fluctuations in the initial wake region are of the same order of magnitude as the mean velocity defect. This is typical for wakes (Tennekes and Lumley, 1974). A clear indication of the wake type flow in the region behind the crest is also found from the measurements of Battjes and Sakai (1980) in a steady breaking wave.

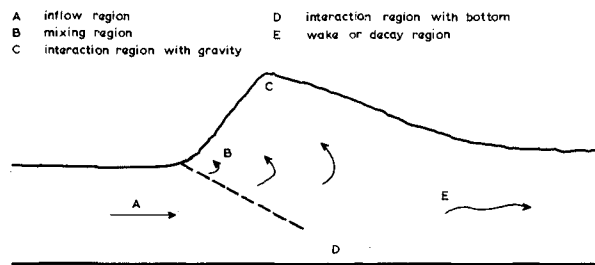


Figure 9a Model of a quasi-steady breaking wave (after Peregrine and Svendsen, 1978) for a reference frame moving with the wave

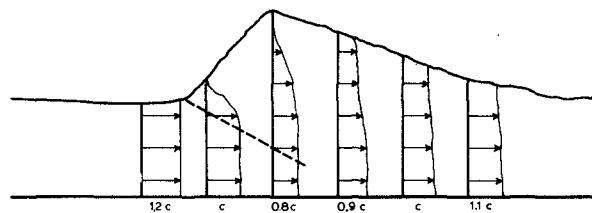


Figure 9b Horizontal velocity field of a quasi-steady breaking wave for a reference frame moving with the wave

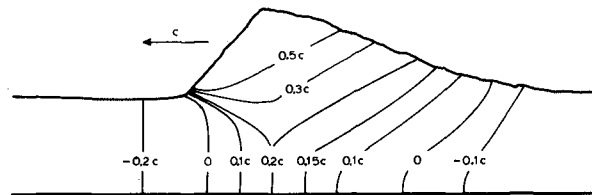


Figure 9c Horizontal velocity field of a quasi-steady breaking wave for a fixed frame of reference

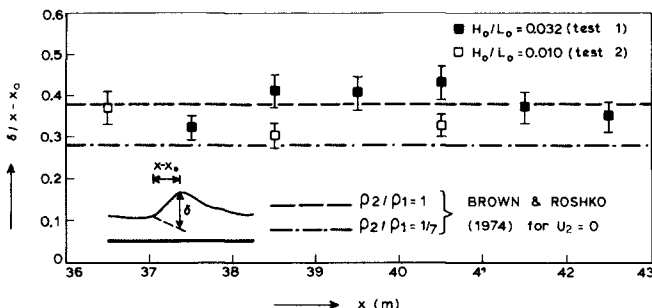


Figure 10 Growth rate of mixing regions

Summarizing, it is concluded that the measured horizontal periodic and turbulent velocity fields are at least in qualitative agreement with the model of a quasi-steady breaking wave as proposed by Peregrine and Svendsen (1978).

##### 5. PRESSURE FIELD

In this paragraph a semi-quantitative description of a typical, measured periodic pressure field of the inner breaking region is presented. As will be shown, the magnitude and gradients of the vertical velocity and the surface elevation control the dynamic pressure field. From the comparison with the theories in §3 it is clear that the cnoidal theory is unable to predict the magnitudes of the velocity field. Linear theory is not able to describe the gradients in the velocity fields and surface elevation. Therefore a quantitative comparison with the cnoidal and linear theory is not considered appropriate at this stage of the study.

In Figure 11a the periodic dynamic pressure  $\bar{p}/\rho g + z$  measured at different levels in the inner region is given, along with the surface elevation or equivalently the dynamic hydrostatic pressure head, i.e. the dynamic pressure head that would result from a hydrostatic pressure distribution. The test conditions differ from the conditions of test I only in the presence of the dummy side wall, which is the cause of a surface elevation profile slightly different from test I. Figure 11b shows the measured periodic vertical velocity at different levels and the surface elevation of test I. The following description is based on the balance of vertical momentum (Dorrestein, 1961). Consider a fixed control volume of length  $\delta x$  extending between a level  $z = z_1$  and the surface  $z = n$ . The dynamic equation reads:

$$(p/\rho g + z) \Big|_{z=z_1} = n - \frac{1}{g} w^2 \Big|_{z=z_1} + \frac{1}{g} \frac{\partial}{\partial t} \int_{z_1}^n w dz + \frac{1}{g} \frac{\partial}{\partial x} \int_{z_1}^n uw dz$$

From the measurements it is concluded that the magnitude of the last term on the right hand side, representing the advective gain of vertical momentum through the side boundaries, is at all times small, i.e. less than 10%, relative to the second and third term. The second term represents the advective gain of vertical momentum through the base of the control volume and the third term represents the gain due to the difference of vertical momentum at time  $t$  and  $t + \delta t$ . These terms are responsible for the deviation of the pressure  $\tilde{p}/\rho g$  from the hydrostatic pressure  $\tilde{\eta} - z$ . A schematic representation of the magnitude and gradients of these two terms is given in Figure 11c in which 3 zones are distinguished. In zone A  $\tilde{w}$  and  $z_1 \int \tilde{w} dz$  are small in magnitude and gradients, resulting in a hydrostatic pressure distribution. In zone B at first a strong gradient in  $z_1 \int \tilde{w} dz$  and small  $\tilde{w}$  result in a pressure higher than the hydrostatic value. The magnitude of  $w$  increases strongly and  $w^2$  tends to cancel out  $\frac{\delta}{\delta t} z_1 \int \tilde{w} dz$ . In zone C both terms contribute negatively to the right hand side of the equation, so at the crest a pressure lower than the hydrostatic pressure results.

The measured periodic pressure field as presented in Figure 11a appeared to be typical not only for the breaking waves of the inner region but also for the breaking waves in the outer region. Nearer to the breaking point the pressure fields show qualitatively the same deviations though more pronounced. The opposite effects are found nearer to the shoreline.

These findings are in agreement with measurements of crest and trough pressure in breaking waves of van Dorn (1976), who found a hydrostatic pressure under the troughs and a pressure lower than hydrostatic pressure under the crests, increasing substantially nearer to the breaking point.

#### 6. INTEGRAL PROPERTIES

As described in the introduction the integral properties are evaluated in the second phase of this study. The planned approach is outlined hereafter and illustrated with a preliminary result for the mean momentum balance.

Time averaging of the vertically integrated density and flux of horizontal momentum and energy yields the so-called integral properties, which enables the following analyses. Firstly, local values of the integral properties can be compared to accepted theoretical expressions. Secondly, a check is possible on the theoretical and measured relation between gradients in the time and depth integrated momentum flux and gradients in the mean water level. Thirdly, the mean energy dissipation can be obtained from gradients in the time and depth integrated energy flux, so that dissipation models can be checked.

To quantify the integral properties the ensemble mean values of  $u$ ,  $p$ ,  $u^2$ ,  $w^2$ ,  $u^3$ ,  $uw^2$  and  $pu$  must be integrated over time and depth. Since  $u$  and  $p$  were not measured simultaneously the term  $pu$  is approximated by  $\tilde{p}\tilde{u}$ , thus neglecting the turbulent  $pu$ -interaction and the joint contribution of waves and turbulence. However, because of the air entrainment velocity measurements were only possible up to lightly aerated regions. For a full time and depth integration it is therefore necessary to make extrapolations in the crest regions of the breaking waves. For the most essential extrapolation of the horizontal velocity  $u$  it is

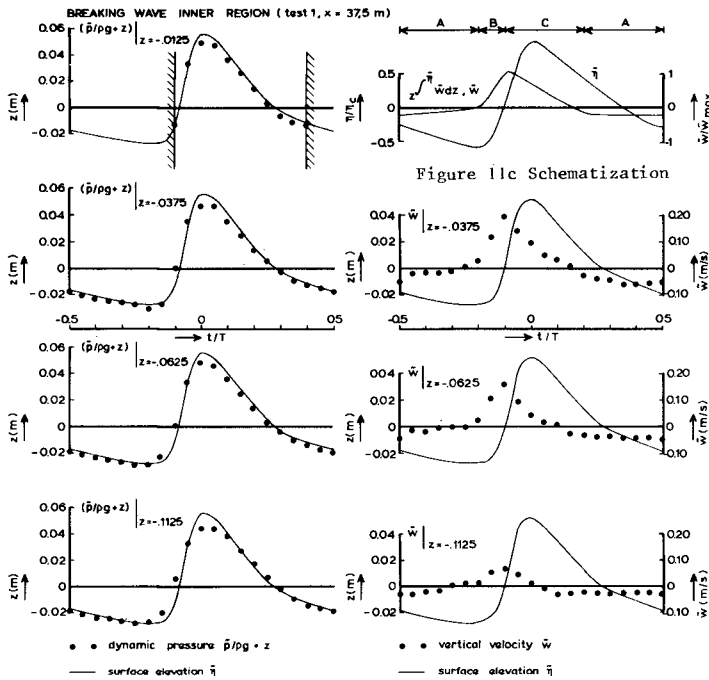


Figure 11a Dynamic pressure distribution

Figure 11b Vertical velocity distribution

possible to use the continuity equation and the constant form assumption - as suggested by the measurements - as follows. For constant form  $\frac{\delta}{\delta t} = -c \frac{\delta}{\delta x}$  so the continuity equation can be written:

$$-c \frac{\delta}{\delta x} \int_{-h}^{\bar{\eta}} \rho u dz + \frac{\delta}{\delta x} \int_{-h}^{\bar{\eta}} \rho u dz = 0$$

Using  $\int_{-h}^{\bar{\eta}} \rho u dz = 0$  it follows:  $\int_{-h}^{\bar{\eta}} \rho u dz = \rho c (\eta - \bar{\eta})$ .

From the measurements the velocity of propagation  $c$  and the surface elevation  $\eta - \bar{\eta}$  are known. The value of the velocity integral so obtained yields a constraint that can be used for the extrapolation. A check on the validity of this expression in the trough regions where  $-h^{\eta} \rho u dz$  can be determined, showed it to be a valid relation.

A preliminary result of the analysis of the integral properties is given by the following evaluation of the mean momentum balance.

For a number of stations in the surfzone the time mean horizontal momentum flux  $I_{xx} = -h^{\eta} (p + \rho u^2) dz$  is determined using the measured (and extrapolated)  $p$  and  $u$ . Gradients in the excess time mean horizontal momentum flux due to the presence of waves or radiation stress induce a variation of mean water level,  $\bar{\eta}$ , as follows from the mean momentum balance (Longuet-Higgins and Stewart, 1962):

$$\frac{dS_{xx}}{dx} + \rho g (h + \bar{\eta}) \frac{d\bar{\eta}}{dx} = 0$$

in which:

$$S_{xx} = I_{xx} - \frac{1}{2} \rho g (h + \bar{\eta})^2$$

The measured mean water level is compared (Fig. 12) with

a) the mean water level calculated from the measured  $I_{xx}$  using the equation above and

b) the mean water level calculated from the measured wave height,  $H_{rms}$ , using the linear approximation of  $S_{xx} = (2n - \frac{1}{2})E$  and the equation above. The comparison shows that a fair agreement exists between the measured mean water level and the mean water level calculated from the measured momentum flux. This is not unexpected because the derivation of the mean water level from the measured momentum flux using the momentum balance is nearly exact, since only the bottom shear stress is neglected. Use of the linear approximation of the radiation stress gives strong deviations in magnitude and gradients of the calculated mean water level around the breaking point.

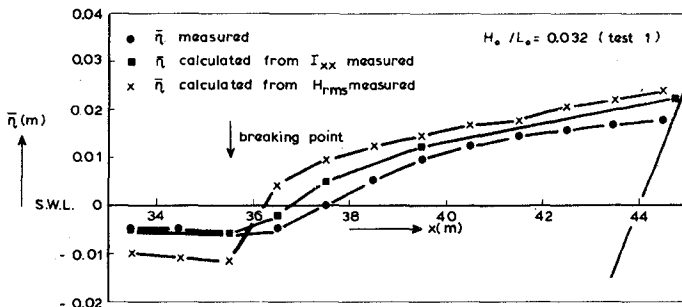


Figure 12 Comparison of measured and calculated mean water level

## 7. CONCLUSIONS

The internal velocity and pressure fields of quasi-steady spilling breaking waves have been investigated experimentally. So far the following conclusions can be drawn:

- The flow fields in the inner breaking region show a similarity not only from point to point for a particular wave condition, but also at corresponding points for different deep water wave conditions (see Fig. 6 and 8). This is a generalisation of the conclusions made by Svendsen et al (1978) on the basis of the similarity of the surface profiles in the inner region.
- A comparison of the horizontal periodic velocity fields with the non-breaking cnoidal (Keulegan & Patterson) and linear theory shows that:
  - a) the cnoidal theory fails to predict the horizontal velocity field qualitatively and quantitatively;
  - b) linear theory predicts the order of magnitude of the maximum and minimum horizontal velocities quite well, which is probably due to the full wave profiles.
- The model of a quasi-steady breaking wave as proposed by Peregrine and Svendsen (1978) is - at least qualitatively - shown to be in agreement with the measured horizontal periodic and turbulent velocity fields.
- The periodic pressure field deviates from hydrostatic pressure at the breaking wave front and at the wave crest. Shortly behind the wave crest and at the trough region the periodic pressure field is hydrostatic. The deviations can be explained semi-quantitatively from the vertical velocity distribution using the vertical momentum balance.
- The integral properties can in principle be quantified from the measured internal velocity and pressure field. This makes a valuable check possible on known relations, such as the mean momentum balance. It also allows for a fundamental study of the energy dissipation.

## 8. ACKNOWLEDGEMENT

This study was suggested by dr. J.A. Battjes as a part of the coastal research program (TOW) of the Public Works Department of the Netherlands (Rijkswaterstaat). The author gratefully acknowledges the encouragement and valuable suggestions of dr. Battjes.

## 9. REFERENCES

- Battjes, J.A. (1975). Modeling of turbulence in the surfzone. Proc. Symp. on Modeling Techniques, San Francisco, p. 1050-1061.
- Battjes, J.A. and Sakai, T. (1980). Velocity field in a breaker. Proc. 17th Coast. Engng. Conf., Sydney.
- Brown, G.L. and Roskho, A. (1974). On density effects and large structure in turbulent mixing layers. J. Fluid Mech., 64, p. 775-816.

- Dean, R.G. (1974). Evaluation and development of water wave theories for engineering application. Special Report No. 1, Coast. Engng. Research Center.
- Dorrestein, R. (1961). On the deviation of the average pressure at a fixed point in a moving fluid from its "hydrostatic" value. *Appl. sci. Res.*, A, 10, p. 384-392.
- Godefroy, H.W.H.E. (1978). Application of the laser doppler velocity measurement method in open and closed conduits. *Proc. Flomeko*, Groningen.
- Hulsbergen, C.H. (1974). Origin, effect and suppression of secondary waves. *Proc. 14th Coast. Engng. Conf. Copenhagen*, chap. 22, p. 392-411.
- Le Méhauté, B., Divoky, D. and Lin, A. (1968). Shallow water waves: a comparison of theories and experiments. *Proc. 11th Coast. Engng. Conf.*, London, chap. 7, p. 86-107.
- Longuet-Higgins, M.S. (1953). Mass transport in water waves. *Phil. Trans. Roy. Soc. London*, A, 903, 245, p. 535-581.
- Longuet-Higgins, M.S. and Stewart, R.W. (1962). Radiation stress and mass transport in gravity waves, with applications to "surf-beats". *J. Fluid Mech.*, 13, p. 481-504.
- Longuet-Higgins, M.S. and Turner, J.S. (1974). An "entraining plume" model of a spilling breaker. *J. Fluid Mech.*, 63, p. 1-20.
- Masch, F.D. and Wiegel, R.L. (1961). Cnoidal waves, tables of functions. Berkely, Calif.: The Engng. Found. Council on Wave Research.
- Peregrine, D.H. and Svendsen, I.A. (1978). Spilling breakers, bores and hydraulic jumps. *Proc. 16th Coast. Engng. Conf.*, Hamburg, chap. 30, p. 540-551.
- Russell, R.C.H. and Osorio, J.D.C. (1958). *Proc. 6th Coast. Engng. Conf.*, USA, Chap. 10, p. 171-183 and appendix by Longuet-Higgins, M.S. The mechanics of the boundary-layer near the bottom in a progressive wave, p. 184-193.
- Svendsen, I.A., Madsen, P.A. and Buhr Hansen, J. (1978). Wave characteristics in the surfzone, *Proc. 16th Coast. Engng. Conf.*, Hamburg, chap. 29, p. 520-539.
- Tennekes, H. and Lumley, J.L. (1972). A first course in turbulence. MIT Press.
- Van Dorn, W.G. (1976). Set-up and run-up in shoaling breakers. *Proc. 15th Coast. Engng. Conf.*, Hawaii, chap. 42, p. 738-751.